





Experimental and Numerical Investigations on a Stone Column in Sandy Ground Contains Clayey Lens

Bazazzadegan, N.¹, Ganjian, N.^{2*} and Nazariafshar, J.²

¹ Ph.D. Candidate, Department of Civil Engineering, Science and Research Branch, Islamic Azad University, Tehran, Iran.

² Assistant Professor, Department of Civil Engineering, Shahr-e-Qods Branch, Islamic Azad University, Tehran, Iran.

© University of Tehran 2024

Received: 02 Oct. 2023;

Revised: 29 Nov. 2023;

Accepted: 02 Jan. 2024

ABSTRACT: Utilizing stone columns proves highly effective in altering the behavior of challenging ground conditions. The combined application of stone columns with surrounding reinforcement enhances the methods efficiency for layered ground formations. The current study investigates the effectiveness and behavior of unreinforced and geotextile-reinforced stone columns integrated into sandy ground containing a soft clayey lens. This problem was investigated employing a Frustum Confined Vessel (FCV) in physical models and using ABAQUS software in numerical analyses. The results of experimental tests, demonstrated that reducing soft lens thickness significantly augmented the bearing capacity of both unreinforced and geotextile-encased stone columns. As soft lens depth increased, both unreinforced and reinforced stone columns exhibited approximately 40% and 10% increases in bearing capacity, respectively. The results of numerical analysis showed that in the presence of soft lens, the change in the length of a stone column had no effect on the occurrence of bulging failure and decreasing placement level of the soft lens, increased the bulging failure occurrence proportional. On the other hand, increasing the thickness of the soft lens reduced the bearing capacity of the ordinary and reinforced stone column. The phenomenon of bulging can occur at the level of the lens placement and up to a depth of about 4 times the diameter of the ordinary column because of existence of a soft lens in a relatively loose sandy bed, while mechanism of failure is not bulging anymore if using encasement.

Keywords: Frustum Confined Vessel (FCV), Stone Column, Bearing Capacity, Clayey Lens, ABAQUS, Reinforcement.

1. Introduction

In the realm of constructing engineered structures like buildings and road embankments, grappling with soft or loose soil beds that display inadequate bearing capacity and susceptibility to settlement exceeding permissible limits remains an

unrelenting challenge. By embedding stone columns within such soil beds, the bearing capacity is augmented, and settlement is curtailed. These columns are effective for reinforcing soft and loose soils to depths of up to 20 meters. The method involves substituting a fraction, ranging from 15% to 35%, of the loose bed volume with gravel

* Corresponding author E-mail: N.Ganjian@srbiau.ac.ir

or crushed stone. This material is meticulously placed within wells of predetermined dimensions, thereby enhancing soil bearing capacity and minimizing settlement. However, the presence of soft lenses within the soil bed introduces complexity. These soft lenses encompass zones of diminished shear strength within the soil matrix, thereby increasing the probability of bulging failure. In many instances, this failure is observed at depths spanning 2 to 3 times the diameter of a stone column. Notably, this failure mode is accentuated in cases where the column length greatly exceeds 4 to 6 times its diameter, particularly within a uniform soil matrix. In regions characterized by the existence of soft lenses, it becomes crucial to bolster soil bearing capacity and mitigate compressibility through the reinforcement of stone columns. This reinforcement strategy is pivotal in evaluating the soft lens is impact on these key parameters.

Moreover, the presence of heterogeneous layers, such as fine-grained strata within sandy beds, contributes to the intricacy of decision-making when assessing the behavior of geotechnical structures. Engineering guidelines (Schaefer et al., 2017), based on valid principles further reveal that the failure mechanism of a stone column in a sandy bed housing an extremely soft lens hinges on the thickness and depth of the lens. Lone et al. (2015) performed experimental studies of the behavior of stone columns by changing the column diameter and length as well as the length and stiffness of the geosynthetic encasement material. They concluded that the bearing capacity of the column increased after encasement with an appropriate geosynthetic in the rigid-base, semi-encased and floating states.

Most studies have reported that bulging failure occurs at a depth of D to $2.5 D$ (D = stone column diameter) from the top of the stone column (Ghazavi and Afshar, 2013; Afshar and Ghazavi, 2014; Mehrannia et al., 2018). Studies on the behavior of stone

columns having different diameters with and without geotextile encasement in layered soil have shown that soil improved by such columns had a greater bearing capacity than did unimproved soil (Prasad et al., 2017). Mohanty and Samantha (2015) conducted experimental and numerical tests on the response of stone columns in layered sand and concluded that the behavior differed in layered and homogeneous soils.

Shamsi et al. (2019) performed experimental and numerical studies of the behavior of sand columns reinforced by vertical geotextile encasement and horizontal geotextile layers. Gu et al. (2020) conducted numerical tests on the bearing capacity of footing supported by geogrid encased stone columns on soft soil.

Nazariafshar et al. (2022) performed experimental studies of the effect of construction method on the performance of ordinary and geotextile-encased stone columns. Danish et al. (2021) by numerical modeling the behavior of stone column in soft clay soil, found that increasing the diameter of the column and the internal friction angle of gravel materials increase the bearing capacity of the stone column.

Also, Pereira et al. (2021) by numerical analyzing a soft embankment that has got improved with a stone column using plaxis and slide software, concluded that the mohr-coulomb behavior model predicts vertical displacements better than the cam-clay behavior model. Saxena and Roy (2022) analyzed the effect of using two different types of gravel materials in the construction of stone columns on the behavior of the column with plaxis software and compared the length and diameter of the stone column in both cases. Hajiazizi and Nasiri (2019) conducted experimental and numerical tests on the stabilizing of reinforced sand slope using geogrid encased stone column. Also, Shahraki et al. (2018) performed studies on the behavior of stone columns in saturated soft grounds using Finite Element (FE) numerical method. Gu et al. (2022) performed model test on the behavior of floating stone columns

reinforced with geogrid encasement. This study, uniquely, investigates the impact of soft lenses on the failure mode and defects in stone columns situated within sandy beds containing such lenses. This examination is driven by excavation logs from northern Iran indicating the presence of layered conditions beneath the surface in specific areas. Here, the results of experimental models in FCV are used to validate the software, and along with, the effect of different parameters on the behavior of a stone column in sandy ground contains clayey lens will be investigated numerically.

2. Experimental Modelling

2.1. Material

The sand used to form the bed was the relatively medium sand from Bandar-e-Anzali in Iran that has a relative density of

60% and a moisture content of about 8%, with other specifications given in Table 1.

To prepare the soft clayey lens, the dry unit weight was set at 80% of the maximum dry density resulting from the standard compaction test (ASTM D 698). Uniaxial compressive strength testing (ASTM D 2166) was conducted on a sample with a 20% moisture content to find out unconfined compressive strength (q_u) of lense. The specifications of the clayey materials are given in Table 2. The materials used for the stone column were crushed stone with a particle size of 2-10 mm, as suggested by Nayak (1983) and Fattah et al. (2011) as presented in Table 3.

Calculating the minimum and maximum dry densities (14.1 and 16.5 kn/m^3 , respectively), the dry unit weight of stone column material was set at 15.7 kn/m^3 , which was equal to a relative density of 70% (Mehran Nia et al., 2018).

Table 1. Properties of bandar-e-anzali sand

Parameters	Unit	Value
Specific gravity (Gs)	-	2.7
Maximum dry unit weight	kn/m^3	15.4
Minimum dry unit weight	kn/m^3	13.3
Internal friction angle (ϕ) at 60% relative density	$^\circ$	32
Dry unit weight for test at 60% relative density	kn/m^3	14.4
Moisture content	%	8
Uniformity coefficient (C_u)	-	1.65
Curvature coefficient (C_c)	-	1.01
Unified soil classification system	-	sp

Table 2. Properties of clay

Parameters	Unit	Value
Specific gravity (Gs)	-	2.67
Maximum dry unit weight	kn/m^3	18.1
Optimum moisture content	%	14.6
Bulk unit weight at 20% water content	kn/m^3	17.4
Plasticity index	%	12
Liquid limit	%	29
Unified soil classification system	-	cld

Table 3. Properties of stone column material

Parameters	Unit	Value
Specific gravity (Gs)	-	2.7
Maximum dry unit weight	kn/m^3	16.5
Minimum dry unit weight	kn/m^3	14.1
Internal friction angle (ϕ) at 70% relative density	$^\circ$	45
Bulk unit weight for test at 70% relative density	kn/m^3	15.7
Uniformity coefficient (C_u)	-	2
Curvature coefficient (C_c)	-	1.23
Unified soil classification system	-	gp

The sand, stone and clay particle size distribution curves resulting from the soil gradation tests (ASTMD 422) are depicted in Figure 1. The reinforcing material specifications were determined based on the scale effect. Considering the similar strain conditions:

$$\varepsilon = \frac{T}{J} = \frac{\sigma_v \cdot k \cdot l}{J} \quad (1)$$

$$\frac{J_{(p)}}{J_{(m)}} = \lambda \quad (2)$$

where ε : is the encasement strain, T : is the tension force per length unit of encasement, J : is the encasement stiffness, σ_v : is the vertical stress, k : is the lateral pressure coefficient, l : is the length of encasement and $1/\lambda$: is the model-to-real-condition scale. The geotextile material stiffness under real conditions is usually less than about 2000 kN/m. In the current study, a scale factor of 1:10 was used based on the scale effect for selection of the reinforcing material stiffness. Specifications of the

geotextile reinforcing material are given in Table 4.

2.2. Experimental Investigation (Frustum Confined Vessel)

Testing of a full-scale model that is conducted on-site produces the best results. However, the heavy cost of full-scale testing and the inability to repeat tests under exactly equal conditions have led to the popularity of small-scale physical model tests. A physical model is, in fact, a smaller version of an actual geotechnical structure.

For small-scale physical modeling of geotechnical structures such as stone columns, the scale selected is usually 1:10 so that the model is not unduly large to complicate working with it and not unduly small to cause a considerable difference in the behavior of the model and the prototype. In conventional small-scale physical models (1 g), limitations concerning stress conditions exist because the stress level is much lower than the actual stress.

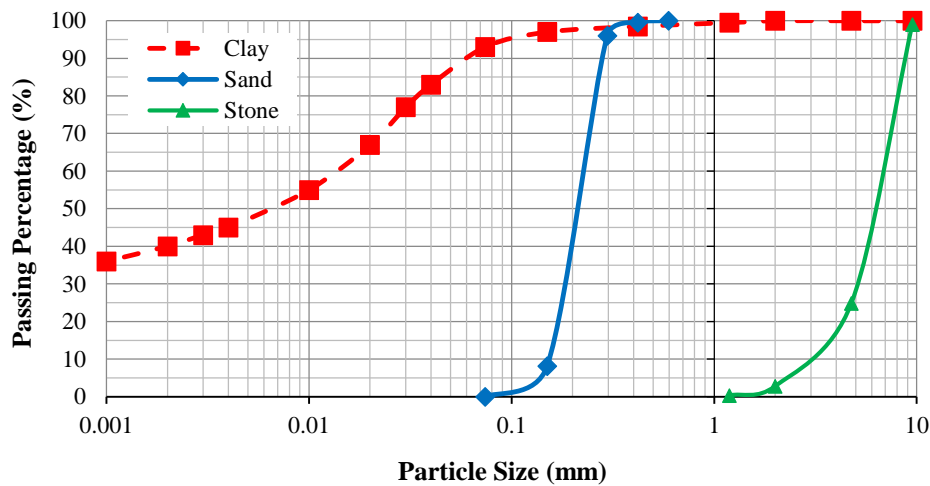


Fig. 1. Particle size distribution of Bandar-e-Anzali sand, clay and stone

Table 4. Properties of geotextile (manufacturer information)

Parameters	Unit	Value
Mass	g/m ²	500
Thickness	mm	3.6
Tensile strength (md)	kn/m	37
Tensile strength (cd)	kn/m	37
Tensile elongation (md)	%	55
Tensile elongation (cd)	%	50
Tensile modulus (md) at 55% tensile elongation	kn/m	67.3
Tensile modulus (cd) at 50% tensile elongation	kn/m	74

In conventional small-scale physical models (1 g), limitations concerning stress conditions exist because the stress level is much lower than the actual stress. Moreover, the small dimensions of a centrifuge model can complicate the installation of measurement tools having fixed volumes and weights, which would, thus, change the soil behavior (Mitchell, 1991). When using an FCV as a part of regular physical modeling (1 g), actual stresses can be applied. The FCV is a container in the shape of a frustum in which the sandy soil layer (bed soil materials) and fine-grained lens are prepared by layer by layer soil compaction.

In the current research, the FCV developed by Jassim et al. (2022) was used for geotechnical modeling. The FCV physical model used as the main container had an upper base diameter of 50 cm, lower base diameter of 170 cm and height of 100 cm. Seling and Mckee (1961) and Chummer (1972) showed that wedge failure occurring under a foundation will extend from the center to the sides up to a distance of 2 - 2.5 times that of the foundation width. In the current study, the distance of container walls to the foundation center was more than 3 times the loading plate width. The stone column had a constant diameter of 80 mm and length of 600 mm (constant length to diameter ratio of 7.5). To prevent deformation of the walls of the FCV boundaries of the physical model, the cylindrical container wall was composed of

a rigid, thick steel sheet. The hydraulic pressure was transferred to the soil from the bottom of the test device through a flexible rubber membrane.

To this end, a compressor transferred compressed air to the air-water tank, thereby forcing the water into the flexible rubber membrane between the bottom of the device and the soil. This transferred the water pressure from the bottom of the device to the soil. Figure 2 is a 3D schematic view of the FCV device showing the dimensions of its parts and physical modeling.

Due to the specific geometrical shape of the container, along with the application of upward vertical pressure proportionate to the actual conditions from the bottom of the frustum, the horizontal stress increased as the depth increased along the device axis. Thus, the stress above the soil surface (in contact with the air) was 0 and increased proportionally as the depth increased. As stated, due to the geometrical shape of the device, the lateral pressure of the soil as a coefficient of the vertical stress and a function of the soil geotechnical properties also increased as the soil depth increased.

This means that the FCV device conditions were similar to the site conditions, which is a considerable advantage over other physical modelling devices. The distribution of vertical stress in the test device was evaluated experimentally (Mitchell, 1991).

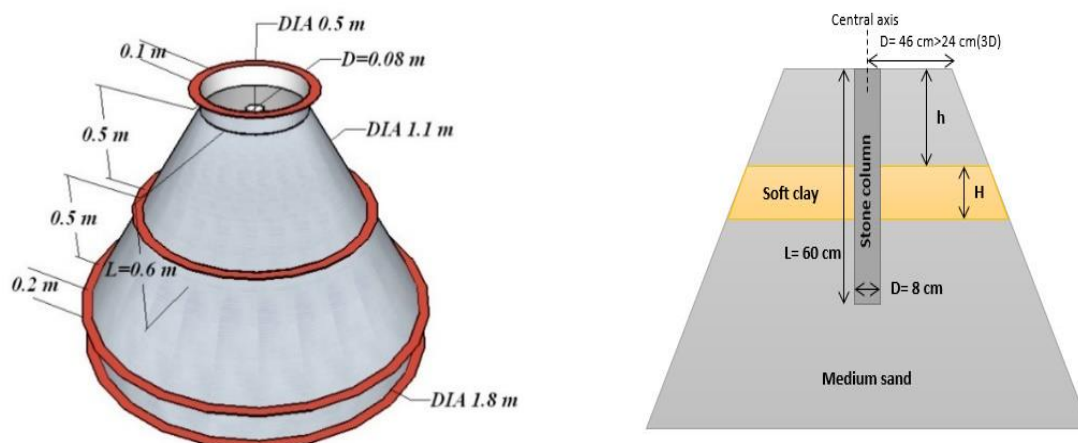


Fig. 2. Schematic profile of FCV and physical modeling

The loading setup comprised the loading device frame, a 5 ton (500 kN) hydraulic load application device and a circular loading plate (foundation) with a diameter of 180 mm. The data measurement system included a regular load cell, miniature load cell and two LVDTs. The data collection and recording system comprised an eight-channel data logger and a laptop (Figure 3). Two LVDTs are placed on the loading plate to record displacement.

A load cell with a capacity of 5000 kg revealed the total force applied to the loading plate. A miniature load cell with a capacity of 500 kg was placed on the stone column to determine the stone column bearing force and the stress distribution on the stone column to determine the stress concentration ratio. Loading was based on the force control with a velocity of 10 kg/min.

The loading plate (diameter of 18 cm and thickness of 3 cm) was made of rigid steel with its center positioned over the center of the stone column. All tests

continued until the loading plate had settled for 45 mm. The capacity and combined error of load cell are 10 tf and 0.03%, although for the miniature load cell these are 500 kgf and 0.15% respectively. LVDT measurement stroke and linearity is also 100 mm and +/- 0.2%, respectively, based on the factory catalogs.

2.3. Experimental Plan

Ten small-scale tests were conducted. Control tests were also carried out to ensure the repeatability and consistency of the results and showed good compatibility between the findings. Table 5 presents a summary of the test plans. The models comprised a stone column with a constant length of 60 cm ($L/D = 7.5$) placed in a sandy bed containing a soft lens. The encased (ESC) and unreinforced (OSC) forms had different thickness to column diameter ratios (H/D) and lens depth to column-diameter ratios (h/D). Figure 2 shows the parameters of physical modeling.



Fig. 3. Overview of FCV apparatus and FCV accessories: a) FCV; b) Load cell; c) Mini-load cell, loading plate; and d) Data logger and laptop

Table 5. Outline of load tests on stone column

Test description	Reinforcement	Lens level (mm)	Lens thickness (mm)
O-200-80	-	200	80
O-200-160	-	200	160
E-200-80	geotextile	200	80
E-200-160	geotextile	200	160
O-280-80	-	280	80
O-280-160	-	280	160
E-280-80	geotextile	280	80
E-280-160	geotextile	280	160
unreinforced	-	-	-
reinforced	geotextile	-	-

3. Experimental Test Results

The load-settlement curves for unreinforced and reinforced stone columns were examined according to the lens placement level (-20 and -28 cm) for soft lenses with thicknesses of 8 and 16 cm and also in the absence of a soft lens. Figures 4 and 5 depict the behavior of unreinforced and reinforced stone columns placed in the sand bed with and without a lens at a level of -20 cm.

Figures 6 and 7 depict this behavior at a level of -28 cm. Comparison of Figures 4 and 5 shows that, when the 8 cm lens was positioned at -20 cm, the ultimate load on the unreinforced column was 42% greater

than that for a lens thickness of 16 cm. The load bearing capacity of the reinforced column with an 8 cm soft lens was about 28% greater than of a 16 cm lens.

For the unreinforced column, the absence of a soft lens compared to the existence of an 8 cm lens at -20 cm in depth increased the bearing of the unreinforced column 2.1 fold and that of the reinforced column by 63%. Furthermore, the absence of a soft lens for the unreinforced column compared to the existence of a 16 cm soft lens at 20 cm in depth increased the bearing of the unreinforced column by 2.9 fold and that of the reinforced column by 2.1 fold.

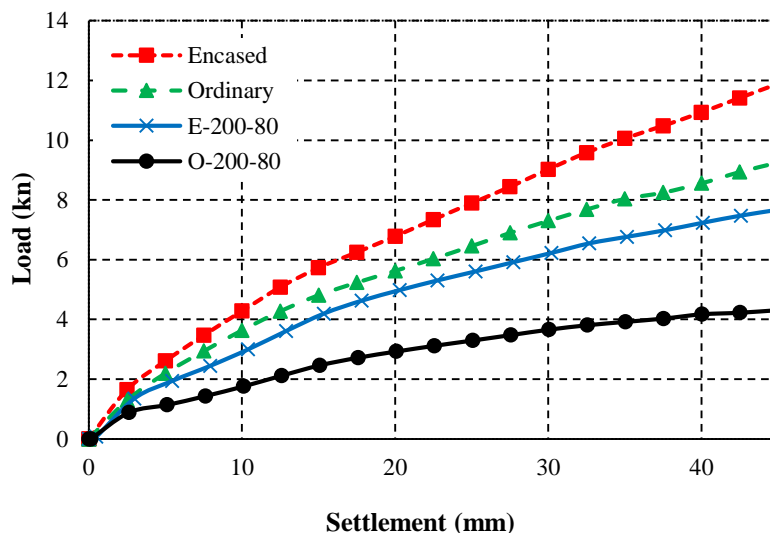


Fig. 4. Load-settlement of reinforced and unreinforced stone column with and without lens with a thickness of 8 cm embedded at -20 cm

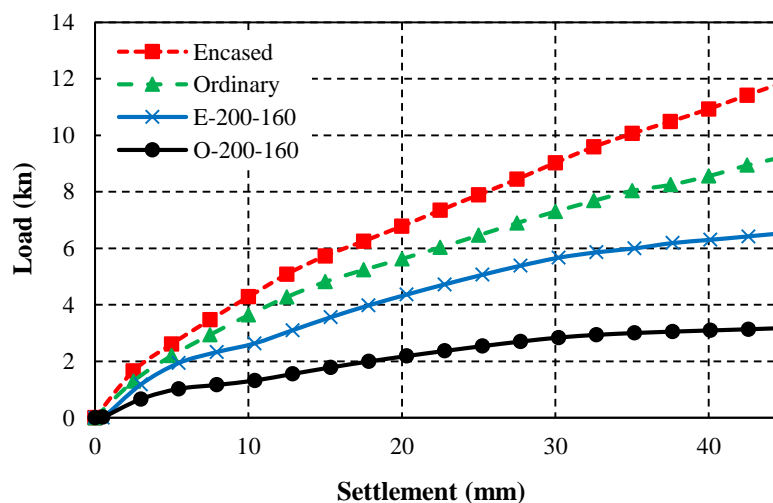


Fig. 5. Load-settlement of reinforced and unreinforced stone column with and without lens with a thickness of 16 cm embedded at -20 cm

Figures 6 and 7 reveal that, when the 8 cm soft lens is located at a depth of -28 cm, the ultimate loading capacity of the unreinforced column was 23% greater than for a 16-cm soft lens at a depth of -28 cm. The load bearing capacity of the reinforced column with an 8 cm soft lens at a depth of -28 cm increased by 11% compared to a 16 cm soft lens at a depth of -28 cm. In soil with no soft lens compared to soil with an 8 cm soft lens at -28 cm in depth, the load bearing capacity of the unreinforced column by increased by 62% and that of the reinforced stone column by 51%. For the unreinforced column, the absence of a soft lens compared to the existence of a 16 cm

soft lens at -28 cm in depth increased the bearing capacity of the unreinforced column 2 fold and that of the reinforced column by 68%.

Compared to the soft lens located at -28 cm in depth, which is outside the possible bulging failure depth, the unreinforced column in soil with a soft lens at -20 cm in depth (the critical bulging failure depth of 2-3 times the diameter of the column) showed 36% lower load bearing capacities for both the 8 cm and 16 cm soft lenses. The reinforced column under similar conditions showed a 16% lower load bearing capacity, on average.

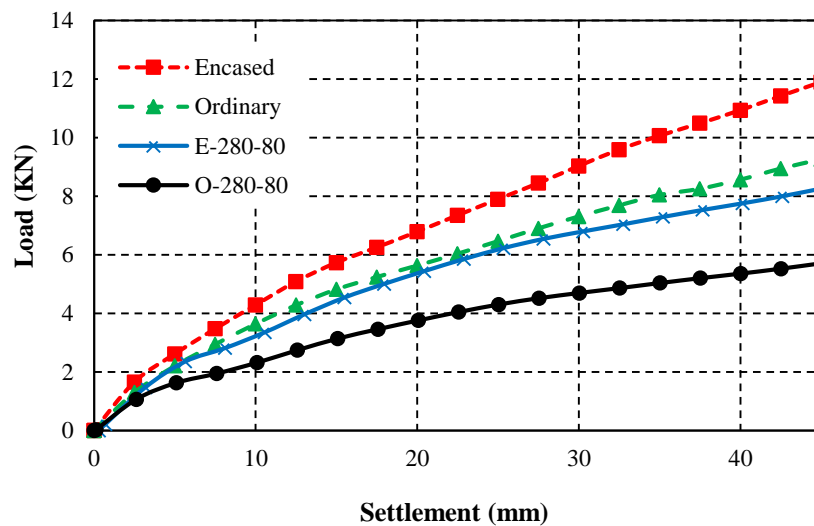


Fig. 6. Load-settlement of reinforced and unreinforced stone column with and without an 8 cm soft lens embedded at -28 cm

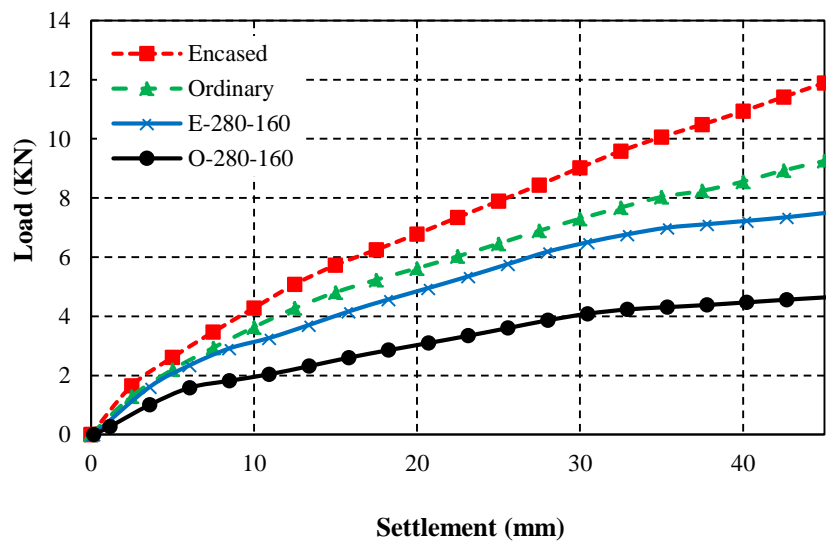


Fig. 7. Load-settlement of reinforced and unreinforced stone column with and without a 16 cm soft lens embedded at -28 cm

4. Numerical Modeling

4.1. Numerical Model Specifications

The current study examined the effect of a soft lens on the failure mode and defects in ordinary and geotextile-encased stone columns located in a saturated sandy bed containing a soft lens using a ABAQUS finite element software. The dimensions of the model are based on the site dimensions of the stone column which are being used in the bed containing the soft lens. The sand used to model the bed is the relatively loose poor graded sand.

Based on the model geometric conditions, axisymmetric modeling has been used. The behavior of sand, clay and stone column materials were also determined based on the Mohr-Coulomb elastic-perfectly plastic failure mode which is widely used for geotechnical analysis and flow law is also assumed to be independent.

The water table is at the same level as the natural ground level and linear elastic behavior is considered for geotextile

materials (Ghazavi and Afshar, 2013, Afshar and Ghazavi, 2014, Mehrannia et al., 2018).

4.2. Model Geometry and Boundary Conditions

Figure 8 is a 2D schematic view of the properties of the axisymmetric model showing the dimensions and materials used for numerical model. The vertical displacement is applied to the rigid plate uniformly and the stone column failure criterion is assumed as 45 cm settlement (vertical displacement) rate in all the analyzed models.

This value is equal to 0.25 of the diameter of the loading plate, which is considered as the ultimate failure limit in some references (Ghazavi and Afshar, 2013). According to the behavior and related failure mechanism, in the stone columns analysis the soil interaction or interface with the stone column and/or geotextile is not considered (Afshar and Ghazavi, 2014).

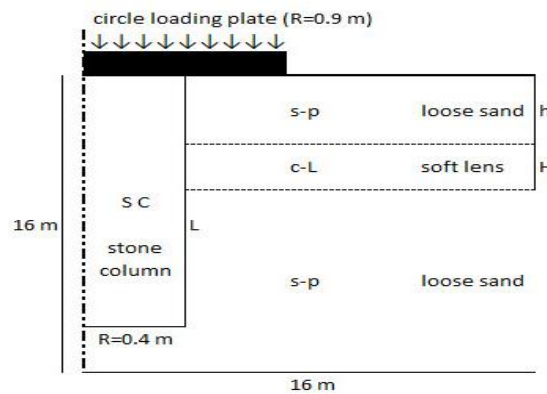


Fig. 8. 2D schematic of model properties

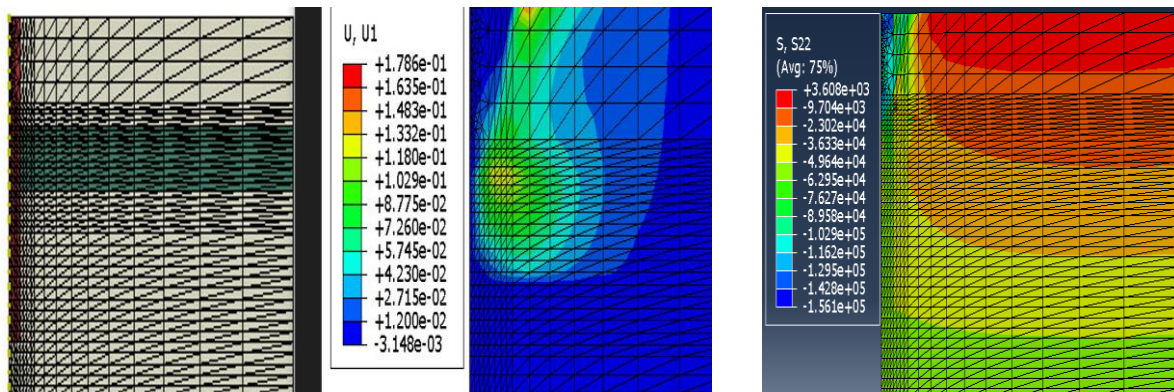


Fig. 9. Meshing of the model in the software, obtained horizontal displacement and vertical stress contours

Figure 9 shows an example of the meshing of the model in the software as well as the horizontal displacement and vertical stress counters in the area of the stone column.

4.3. Numerical Model Investigated and Validation

6 numerical models were analyzed on the whole, which 3 models were ordinary and 3 models were reinforced. In these models, a stone column with three lengths of 600, 800 and 1000 cm also a soft clay lens in level of -200 cm with thicknesses of 120 cm are considered. The analyzed models have been investigated on failure mode (bulging) and bearing capacity of the stone column. Conform to the conditions of the numerical models two physical models were also built with a scale of 1:10 in the FCV (Sedran, 1999) and the results were used to validate and calibrate the results of

the numerical models. Considering the scale effect, the results of two physical models have been used to validate the results of numerical modeling. The materials specifications defined in the validation models are not similar to the same materials defined in the numerical models. Figures 10 and 11 show the load-settlement curves obtained from physical and numerical models with similar conditions, respectively.

5. Numerical Results

To illustrate the effect of stone columns length on the behavior of them, three different lengths of 600, 800 and 1000 cm have been assumed for the stone column and the behavior of the unreinforced and reinforced column with geotextile in variable states of alignment and thickness of the soft lens has been investigated.

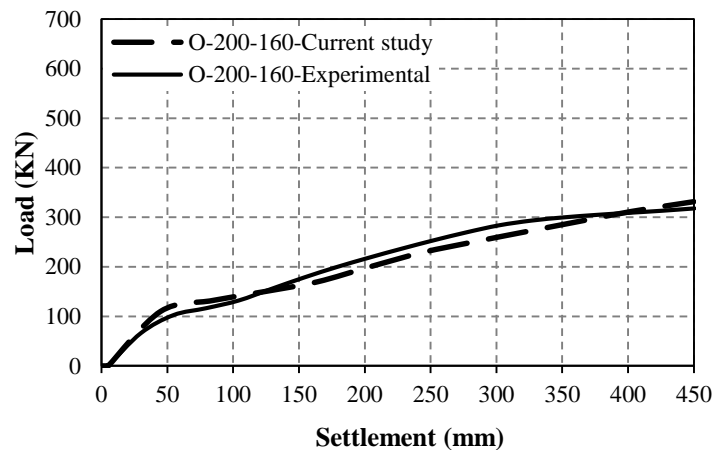


Fig. 10. Load-settlement of ordinary stone column in lens with a thickness of 160 cm embedded at -200 cm

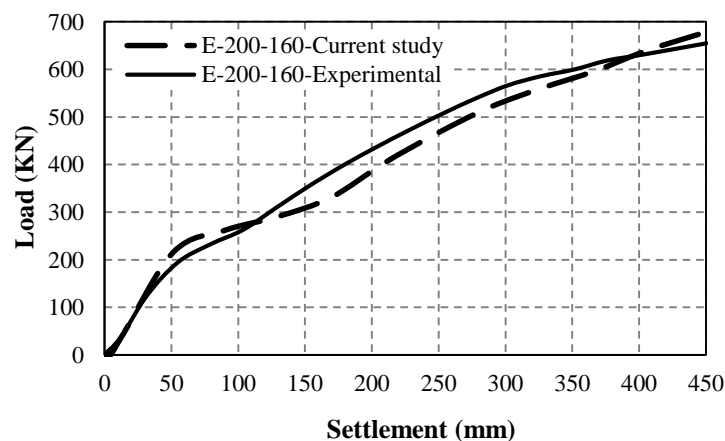


Fig. 11. Load-settlement of reinforced stone column in lens with a thickness of 160 cm embedded at -200 cm

It can be seen in Figures 12 and 13 that changing the length of the column has no effect on the maximum lateral displacement (bulging) and the failure of the stone column, and the stone column with different lengths suffers bulging failure in the range of soft lens placement. Moreover, reinforcing stone column with geotextile has reduced the maximum bulging by 60%.

Furthermore, based on Figures 14 and

15, it can be seen that, due to the occurrence of bulging, changing the length of the column did not affect its bearing capacity, and increasing the length of the stone column did not increase its bearing capacity. It is clear that, reinforcing stone column with geotextile increases the bearing capacity of the stone column by 32%.

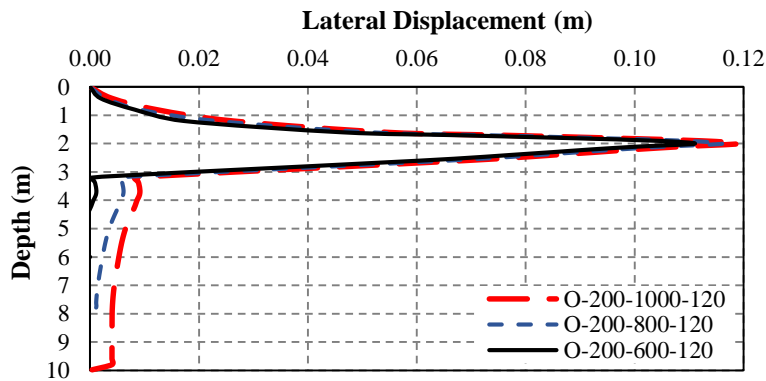


Fig. 12. Lateral displacement along ordinary stone column with a thickness of 120 cm embedded lens at -200 cm level

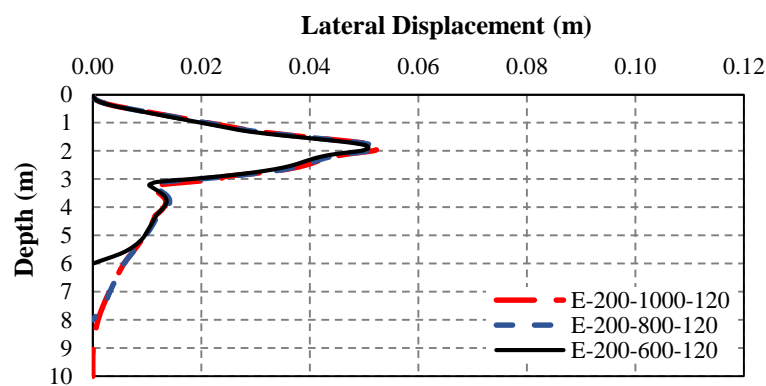


Fig. 13. Lateral displacement along reinforced stone column with a thickness of 120 cm embedded lens at -200 cm level

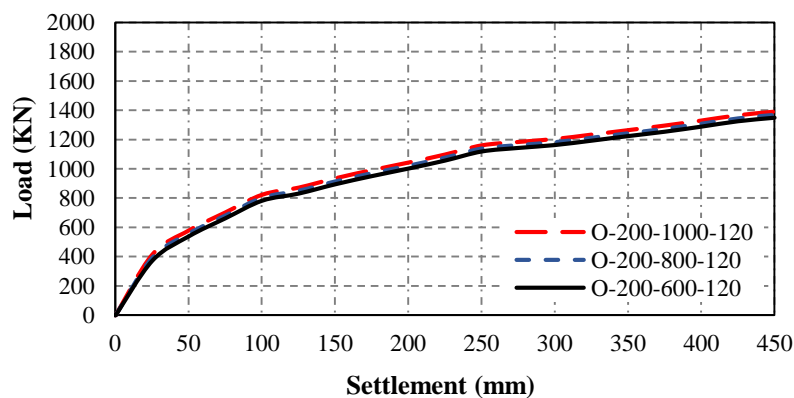


Fig. 14. Load-settlement of ordinary stone column with a thickness of 120 cm embedded lens at -200 cm

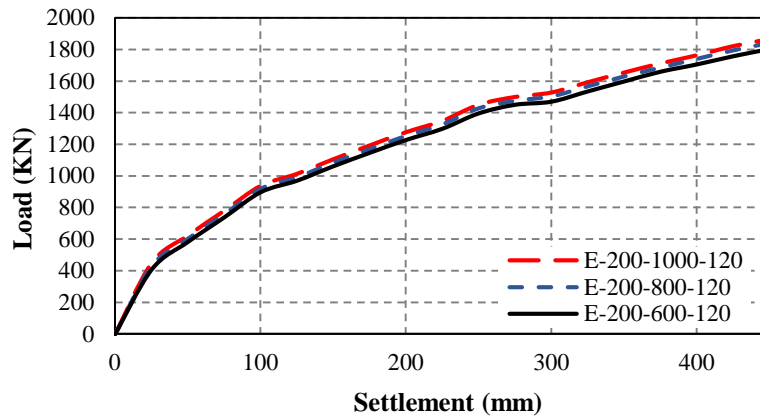


Fig. 15. Load-settlement of reinforced stone column with a thickness of 120 cm embedded lens at -200 cm

6. Conclusions

The experimental investigation represents the inaugural effort to analyze the behavior of stone columns, both with and without reinforcement, situated in sandy ground containing a soft weak lens. This investigation was conducted experimentally utilizing a FCV and also numerically using ABAQUS software. The outcomes gleaned from the load-settlement graphs have yielded the ensuing findings:

- The presence of a soft lens at depths ranging from 1 to 4 times the diameter of the column substantially reduced the bearing capacity of the columns. Notably, a 16 cm thickness of the soft lens accentuated this adverse effect more prominently compared to a 8 cm thickness. The augmentation in bearing capacity for the unreinforced stone columns exhibited an almost twofold increase with diminishing soft lens thickness, surpassing the enhancement observed in the reinforced stone columns.

- A 8 cm clayey lens positioned at a depth of -20 cm led to a twofold decrease in the bearing capacity of both unreinforced and reinforced stone columns. Conversely, when a soft lens was located at -28 cm in depth, the bearing capacity of the stone columns witnessed a 16% increment.

- Elevating the thickness of the soft lens from 8 to 16 cm at a depth of -20 cm precipitated a decline in bearing capacity, affecting unreinforced and reinforced stone columns by approximately 42% and 27%,

respectively. Nevertheless, at a depth of -28 cm, augmenting the soft lens thickness translated to a 23% and 11% rise in bearing capacity for unreinforced and reinforced stone columns, respectively.

- With the existence of soft lens increasing the length of the stone column has no effect on reducing the maximum radial displacement and its failure mode. Also, the stone column with different lengths, with the existence of soft lens has bulging failure.

- With the existence of soft lens, increasing the length of the stone column has no effect on increasing of bearing capacity, and increasing the length of the stone column does not increase its bearing capacity. Only reinforcing stone column with geotextile increases the bearing capacity. According to the results of this research, if stone columns are used to improve ground where there is a possibility of very weak lenses in a depth of less than 5 meters from the surface of the earth, special considerations should be taken into account in the design of stone columns. In these cases, it is recommended to use an encasement stone column to prevent bulging failure.

7. References

- Afshar, J.N. and Ghazavi, M. (2014). "Experimental studies on bearing capacity of geosynthetic reinforced stone columns", *Arabian Journal for Science and Engineering*, 39, 1559-1571, <https://doi.org/10.1007/s13369-013-0709-8>.
- Chummar, A. (1972). "Bearing capacity theory from

- experimental results", *Journal of the Soil Mechanics and Foundations Division*, 98(12), 131-1324-1, <https://doi.org/10.1061/JSFEAQ.0001816>.
- Danish, A., Taib, S.N.L., Ayadat, T. and Hasan, A. (2021). "Numerical investigation on the performance of stone columns under raft foundation in soft clayey soils", *IOP Conference Series, Materials Science and Engineering*, IOP Publishing, 1101, 012015, <https://10.1088/1757-899X/1101/1/012015>.
- Fattah, M.Y., Shlash, K.T. and Al-Waily, M.J.M. (2011). "Stress concentration ratio of model stone columns in soft clays", *Geotechnical Testing Journal*, 34(1), <http://doi.org/10.1520/GTJ103060>.
- Ghazavi, M. and Afshar, J.N. (2013). "Bearing capacity of geosynthetic encased stone columns", *Geotextiles and Geomembranes*, 38, 26-36, <https://doi.org/10.1016/j.geotexmem.2013.04.003>.
- Gu, M., Han, J. and Zhao, M. (2020). "Three-dimensional DEM analysis of axially loaded geogrid-encased stone column in clay bed", *International Journal of Geomechanics*, 20(3), 04019180, [https://doi.org/10.1061/\(ASCE\)GM.1943-5622.0001595](https://doi.org/10.1061/(ASCE)GM.1943-5622.0001595).
- Gu, M., Mo, H., Qiu, J., Yuan, J. and Xia, Q. (2022). "Behavior of floating stone columns reinforced with geogrid encasement in model tests", *Front Mater*, 9, 980851, <https://doi.org/10.3389/fmats.2022.980851>.
- Hajiazizi, M. and Nasiri, M. (2019). "Experimental and numerical investigation of reinforced sand slope using geogird encased stone column", *Civil Engineering Infrastructures Journal*, 52(1), 85-100, <https://doi:10.22059/cej.2019.253069.1468>.
- Jassim, A., Ganjian, N. and Eslami, A. (2022). "Design and fabrication of frustum confining vessel apparatus for model pile testing in saturated soils", *Innovative Infrastructure Solutions*, 7(5), 1-11, <http://doi.org/10.1007/s41062-022-00877-x>.
- Lone, U.R., Dar, M.H. and Ahanger, M.Y. (2015). "Effect of l/b ratio of stone column on bearing capacity and relative settlement of sandy soil (an experimental study)", *International Journal of Civil Engineering and Technology*, 6(1), 55-61, https://iaeme.com/masteradmin/journal_uploads/ijci-et/volume6issue1/ijci-et0601007.pdf.
- Mehranian, N., Kalantari, F. and Ganjian, N. (2018). "Experimental study on soil improvement with stone columns and granular blankets", *Journal of Central South University*, 25, 866-878, <https://doi.org/10.1007/s11771-018-3790-z>.
- Mitchell, R. (1991). "Centrifuge modelling as a consulting tool", *Canadian Geotechnical Journal*, 28(1), 162-167, <https://doi.org/10.1139/t91-018>.
- Mohanty, P. and Samantha, M. (2015). "Experimental and numerical studies on response of the stone column in layered soil", *International Journal of Geosynthetics and Ground Engineering*, 1(27), 1-14, <https://doi.org/10.1007/s40891-015-0029-z>.
- Nayak, N. (1983). "Recent advances in ground improvements by stone column", *Proceedings of Indian Geotechnical Conference*, Madras, IGC 83, <https://www.issmge.org/uploads/publications/1/33/1989020155.pdf>.
- Nazariafshar, J., Shafiee, A. and Mehrannia, N. (2022). "Effect of construction method on the performance of ordinary and geotextile-encased stone columns", *Iranian Journal of Science and Technology, Transactions of Civil Engineering*, 46, 4751-4761, <https://doi.org/10.1007/s40996-022-00888-9>.
- Pereira, P.G.D.S., Pachenco, M.P. and Lima, B.T. (2021). "Numerical analysis of soft soil improved with stone column technique", *REM-International Engineering Journal*, 74, 319-327, <https://doi.org/10.1590/0370-44672020740062>.
- Prasad, S.S.G., Vasavi, C. and Sai, K.P. (2017). "Behavior of stone column in layered soils using geotextile reinforcement", *International Journal of Civil Engineering*, 8(8), 453-462, https://www.academia.edu/34738935/behaviour_of_stone_column_in_layered_soils_using_geotextile_reinforcement.
- Saxena, S. and Roy, L.B. (2022). "Suitability analysis of stone column materials with plaxis", *Engineering, Technology and Applied Science Research*, 12(2), 8421-8425, <https://doi.org/10.48084/etasr.4761>.
- Schaefer, V., Berg, R., Collin, J., Christopher, B., DiMaggio, J., Filz, G., Bruce, D. and Ayala, D. (2017). *Ground modification methods-reference manual-volume ii*, US Department of Transportation Federal Highway Administration, Washington, DC, USA, <https://geotechnical-library.geotill.com/ground-modification-methods-reference-manual-volume-ii-fhwa-nhi-16-028.pdf>.
- Sedran, G. (1999). "Experimental and analytical study of a frustum confining vessel", <http://hdl.handle.net/11375/6498>.
- Selig, E. and Mckee, K. (1961). "Static and dynamic behavior of small footings", *Journal of the Soil Mechanics and Foundations Division*, 87(6), 29-45, <https://doi.org/10.1061/JSFEAQ.0000378>.
- Shahraki, M., Rafiee-Dehkharghani, R. and Behnia, K. (2018). "Three-dimensional finite element modeling of stone column-improved soft saturated ground", *Civil Engineering Infrastructures Journal*, 51(2), 389-403, <https://doi.org/10.7508/cej.2018.02.009>.
- Shamsi, M., Ghanbari, A. and Nazariafshar, J. (2019). "Behavior of sand columns reinforced by vertical geotextile encasement and horizontal geotextile layers", *Geomechanics and Engineering*, 19(4), 329-342, <https://doi:10.12989/gae.2019.19.4.329>.



This article is an open-access article distributed under the terms and conditions of the Creative Commons Attribution (CC-BY) license.